



## Seismicity and outgassing dynamics of Nyiragongo volcano

Julien Barrière<sup>a,\*</sup>, Nicolas d'Oreye<sup>a,b</sup>, Adrien Oth<sup>a</sup>, Nicolas Theys<sup>c</sup>, Niche Mashagiro<sup>d</sup>,  
Josué Subira<sup>d</sup>, François Kervyn<sup>e</sup>, Benoît Smets<sup>e</sup>

<sup>a</sup> European Center for Geodynamics and Seismology (ECGS), Walferdange, Luxembourg

<sup>b</sup> National Museum of Natural History (NMNH), Walferdange, Luxembourg

<sup>c</sup> Royal Belgian Institute for Space Aeronomy (BIRA-IASB), Uccle, Belgium

<sup>d</sup> Goma Volcano Observatory (GVO), Goma, D.R. Congo

<sup>e</sup> Royal Museum for Central Africa (RMCA), Tervuren, Belgium

### ARTICLE INFO

#### Article history:

Received 25 April 2019

Received in revised form 23 August 2019

Accepted 5 September 2019

Available online xxxx

Editor: T.A. Mather

#### Keywords:

volcano  
Nyiragongo  
lava lake  
seismology  
outgassing  
SO<sub>2</sub>

### ABSTRACT

Active lava lakes at volcanoes can be regarded as open windows to their magmatic systems. The dynamics of such lakes may therefore provide decisive insights into deeper magmatic processes, potentially leading to fundamental theoretical implications and volcano monitoring improvements. Among the rare volcanoes on Earth hosting a persistent lava lake, Nyiragongo in D.R. Congo directly threatens a massive population of roughly 1 million inhabitants. Here we analyze close-range (i.e., summit) and distant (around 17 km) seismic measurements acquired at this African volcano between 2011 and 2018 in order to better understand the seismic signature of the lava lake activity and how it relates to the deeper volcanic processes. Both summit and distant seismic records contain a similar continuous tremor pattern attributable to the lava lake activity. Combining this information with time-lapse camera images and lava lake level measurements confirms the mechanism of gas pistoning at Nyiragongo, which is characterized by short-duration (a few minutes long) and meter-scale level variations during the period of observation. We also characterize the dominant periodicity of this shallow tremor signature of about a few tens of minutes. Because this marked periodic pattern varies during a significant one-month fluctuation of SO<sub>2</sub> emissions (estimated from space), we suggest that this particular seismic periodicity corresponds to the convective lake movement driven by the persistent degassing typical of active open-vent volcanoes. Finally, new seismic evidence reveals the effect of deep magmatic intrusion and consequent major pressure changes in the plumbing system, resulting in sudden and large drops of the lava lake level associated with strong degassing. Such transient episodes have similar characteristics to total lava lake drainage associated with flank eruptions already observed at this volcano in 1977 and 2002, or at Kīlauea volcano in 2018.

© 2019 Elsevier B.V. All rights reserved.

### 1. Introduction

At volcanoes with lava lakes of decadal persistence, the lava lake activity described by geophysical observations at the summit (e.g., level, degassing, thermal anomaly, seismicity) often exhibits some repeatable patterns (e.g., Lev et al., 2019) that are generally explained by variable deep processes, such as regular pulsating batches of deep-sourced bubbly magma at Erebus, Antarctica (Molina et al., 2015); variable convective regimes driven by instabilities of magma flow inside or entering the lake at Erta 'Ale, Ethiopia (Jones et al., 2006); gas pistoning due to foam collapse at the top of the magma conduit feeding the Halema'uma'u lava lake

at Kīlauea, Hawaii (Chouet and Dawson, 2015); or foam collapse at the roof of the shallow magma chamber at Kīlauea's Pu'u 'Ō'ō and Mauna Ulu craters (Vergnolle and Jaupart, 1990). Aside from these "deep models", Patrick et al. (2016a, 2016b) proposed a very shallow mechanism of gas trapping at the top of the lake in order to explain gas pistoning and spattering observations at Halema'uma'u.

Belonging to this small family of active lava lakes of high longevity, Nyiragongo volcano is located in the Virunga Volcanic Province (VVP) in D.R. Congo and has been relatively understudied since the first geophysical expedition to its summit in 1959 (de Magnée, 1959). In recent years, however, several scientific expeditions taking visual/thermal camera images (Burgi et al., 2014; Smets et al., 2017; Spampinato et al., 2013; Valade et al., 2018), degassing measurements (Bobrowski et al., 2016, 2017; Sawyer et al., 2008) or infrasound records (Valade et al., 2018) took place in Nyiragongo's crater. Surface observations provided some clues

\* Corresponding author.

E-mail address: julien.barriere@ecgs.lu (J. Barrière).

**Table 1**  
Hardware installed in each seismic station. Manufacturers of ESPC, Trillium and LE3D sensors are Güralp, Nanometrics and Lennartz, respectively. DM24 and Centaur are Güralp and Nanometrics datalogger, respectively. GAIA is a digitizer system developed by INGV (Istituto Nazionale di Geofisica e Vulcanologica, Italy). The periods analyzed in this study and the corresponding figures are also indicated.

Station name (location)	Period of use (analyzed in this study)	Figures	Seismic sensor & corner period	Datalogger
Nyiragongo	17–20 Sept. 2011	2, 3, 4, 5	ESPC 60 s	DM24
	1 March–30 Nov. 2018	2, 5, 6	Trillium 120 s	Centaur
Bulengo	3 June 2011	8	LE3D 5 s	GAIA
	17–20 Sept. 2011	2, 3, 4, 5		
	12 Nov. 2016	8		
	1 March–30 Nov. 2018	2, 5, 6	Trillium 120 s	Centaur

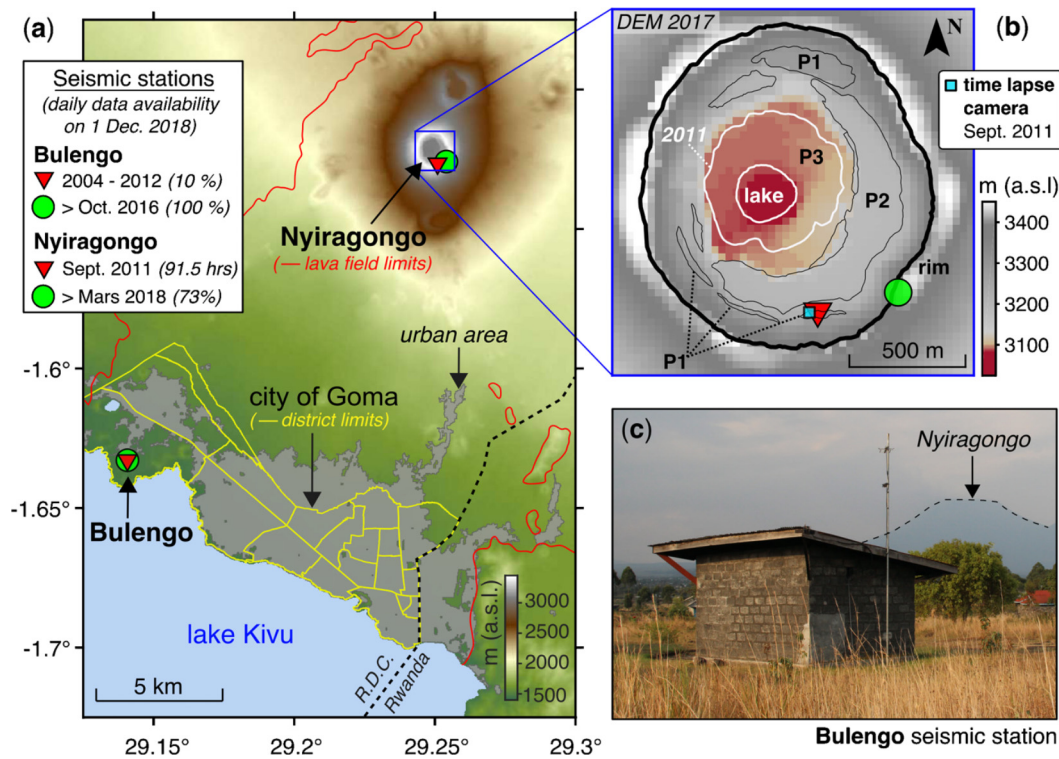


**Fig. 1.** (a) Map depicting Nyiragongo volcano (and its associated lava field limits, red line) and the seismic stations installed at the locality of Bulengo and at the summit of Nyiragongo. The district limits (yellow line) of Goma and the extent of the urban area (estimated in 2013) are plotted according to the study of Michellier et al. (2016). The DEM (Digital Elevation Model) used is SRTM 30-m resolution. Red inverted triangles correspond to temporary installations (now dismantled) and green circles are permanent stations (operational at the time of writing). (b) Zoom in the DEM inside Nyiragongo's crater obtained from a photogrammetric survey performed in June 2017, then combined with the 30-m resolution STRM. The crater topography is characterized by the presence of three platforms here called P1, P2, P3. P1 and P2 are formed by slabs of solidified lava lake that remained after its drainage during former eruptions while the deepest platform P3, created after the last eruption in January 2002, has evolved regularly due to the lava lake's overflows (Smets, 2016). The main contours of platforms P1, P2 and P3 are drawn as light black lines and the thick black line represents the rim of the main crater. The white lines correspond to the limits of P3 and the lava lake in September 2011. The sensor location at Nyiragongo is slightly different between 2011 (red triangle) and 2018 (green circle) and spaced by about 140 m along the vertical direction. (c) Picture of the seismic station installed at Bulengo (~17 km away from the summit), whose location remained unchanged between 2011 and 2018 (credit: N. d'Oreye, 26 Sept. 2015). (For interpretation of the colors in the figure(s), the reader is referred to the web version of this article.)

about periodic fluctuations of the lake level (Smets et al., 2017), thermal activity (Spampinato et al., 2013) or plate velocity (Valade et al., 2018). Stable gas measurements spanning time periods of several years (Sawyer et al., 2008) or decades (Le Guern, 1987) as well as noticeable variations linked to a sudden fluctuation of the lake level (Bobrowski et al., 2017) have been also provided. All together, these studies help to better gauge the shallow and deep outgassing mechanisms at Nyiragongo. However, no digital seismic measurement has been reported in the literature at Nyiragongo's summit as yet to our knowledge, although this component is of significant importance in the field of volcanology. In turn, the connection between the dynamics of the lava lake and the behavior of the plumbing system remains poorly understood. We address this question here using a multi-disciplinary approach consisting of close-range (i.e., Nyiragongo's summit) and distant seismic obser-

vations, time-lapse camera images and daily space-based estimates of  $\text{SO}_2$  emissions of the lava lake.

## 2. Geophysical observations used in this study (2011–2018)

### 2.1. Preliminary remarks about the seismic measurements

The main time periods studied here are three days in 2011 (17–19 September 2011) and nine months in 2018 (March to November 2018). Seismic data from the specific days of 3 June 2011 and 12–13 November 2016 are also analyzed. The four different sensors exploited in this study are distributed among two locations, Nyiragongo's crater and Bulengo, the latter being a rural place situated about 17 km SW from the summit on the shore of the Lake Kivu (see Table 1 and Fig. 1).

Prior to the recent deployment of the local seismic network KivuSNet, fully operational since 2015/2016 (Oth et al., 2017), the seismic monitoring infrastructure was restricted to few temporary or permanent analog stations (Hamaguchi et al., 1982, 1992) until 2004. Between 2004 and 2012, 7 digital stations were installed (Pagliuca et al., 2009), leading to the first network of the Goma Volcano Observatory (GVO). We exploit some of these old digital archives, the use of which has been rather limited in the past for studying the volcanic activity (e.g., Pagliuca et al., 2009; Mavonga, 2010; Smets et al., 2014) mostly due to technical issues (e.g., telemetry drop outs or digitizers failures). Moreover, the information about the settings of the digitizer installed at Bulengo in 2011 has been unfortunately lost, which prevents adequate correction of instrumental response. Nonetheless, all sensors have a flat frequency response above 0.25 Hz, which is a prerequisite for our study since the lava lake generates seismic tremor with dominant frequency content above 0.3 Hz (Barrière et al., 2017, 2018). For this reason and for the sake of a consistent analysis between the 2011 and 2018 records (all sampled at 50 Hz), we do not correct for the instrumental transfer function but, instead, we analyze raw waveforms from each seismometer (in digital counts) after applying standard pre-processing (i.e., demeaning, detrending and filtering).

## 2.2. Expedition in September 2011 (seismic and time-lapse images)

In September 2011, several co-authors of this study led an 11-day expedition to Nyiragongo's summit. The primary objective of this mission was to take a series of photogrammetric measurements for detecting morphological changes of the crater as well as monitoring the lava lake level with high-temporal resolution using a Stereographic Time-Lapse Camera (STLC) system (Smets, 2016). The STLC consists of two synchronized time-lapse cameras that acquire stereo-pairs of photographs for the creation of time series of 3D point clouds at regular interval (here, 2 min), thus allowing for the first measurements of lava lake fluctuations at Nyiragongo with high temporal resolution between 18 Sept. 2011 10:51 and 20 Sept. 2011 08:48 UTC (Smets et al., 2017). Synchronous broadband seismic data were recorded with a sensor installed on the same inner platform (called P1, see Fig. 1b) between 16 Sept. 09:30 and 20 Sept. 05:00 UTC. At that time, three digital seismic stations from the former GVO's network functioned, but only records from the Bulengo station fulfilled data completeness and quality criteria for comparison with crater measurements (see Supplementary Text S1 and Fig. S1).

## 2.3. Permanent monitoring in 2018 (seismic and SO<sub>2</sub> emissions)

The two permanent seismic stations "Bulengo" and "Nyiragongo" are part of the local broadband seismic network KivuSNet. Bulengo has a nearly complete data archive since its upgrade in October 2016. Due to the volatile political situation (i.e., Kivu conflict since 2004) and technical difficulties, a permanent seismic station at Nyiragongo's summit has been installed only since March 2018, near the main crater rim (Fig. 1b). Data from both stations are telemetered via cellular network in near real-time.

In addition to seismic observations in 2018, we exploit satellite measurements of SO<sub>2</sub> from the TROPospheric Monitoring Instrument (TROPOMI), launched in October 2017 on the Sentinel-5 Precursor platform. The SO<sub>2</sub> vertical column density is retrieved from each earthshine radiance spectrum using the operational algorithm described by Theys et al. (2017). In order to obtain results that are representative of SO<sub>2</sub> emission plumes in the VVP, the vertical columns are calculated for a fixed SO<sub>2</sub> plume height of 4 km above sea level. For a latitude-longitude box (4°S–1°N, 26–31°E) covering the VVP, the total SO<sub>2</sub> mass is used to monitor the daily

volcanic emissions from Nyiragongo. To do so, all pixels in this box with vertical columns above 1 Dobson Unit (DU) are selected (1 DU =  $2.69 \times 10^{16}$  mol/cm<sup>2</sup>), converted in kilotons and summed while, during this step, isolated pixels are excluded. A similar approach was performed using OMI data in a recent study (Barrière et al., 2017).

Here the use of TROPOMI SO<sub>2</sub> data has three decisive advantages for tracking subtle changes in degassing: (1) it completely covers the VVP region on a daily basis, (2) it improves the detection limit of OMI to SO<sub>2</sub> emissions by a factor 4 (Theys et al., 2019) and (3) it enables the discrimination on a daily basis of the volcanic SO<sub>2</sub> sources thanks to the spatial resolution of TROPOMI of  $3.5 \times 7$  km<sup>2</sup> (Nyiragongo and its neighbor, the active volcano Nyamulagira, are only 13 km from each other). The latter point is of crucial importance and allows to confirm that the TROPOMI SO<sub>2</sub> data used here (March–November 2018) are a direct proxy for the Nyiragongo's lava lake outgassing, disregarding Nyamulagira's source (see Text S2 and Fig. S2).

## 3. Results: the lava lake's seismic tremor

### 3.1. A persistent seismic source

Fig. 2a depicts two pictures of the lava lake taken from the crater's rim spanning a time difference of 6<sup>1/2</sup> yr between 2011 and 2018. Since early March 2016, an eruptive cone has developed on platform P3. The level of P3 has increased asymmetrically by ~20–40 m between September 2011 and March 2018, mostly due to the cone activity since 2016 because lava flows inundate the crater floor. In Figs. 2b and 2c, 3 days of seismic recordings and corresponding spectrograms are plotted for the stations at Nyiragongo's summit and Bulengo, respectively.

Each record shows a continuous tremor pattern attributed to the lava lake activity above 0.3 Hz (Barrière et al., 2017, 2018). At Nyiragongo's summit, this tremor covers almost the entire frequency band up to 10 Hz (see also Fig. S1) but has dominant amplitude values for frequencies below 2 Hz in 2011. In 2018, distinct tremor signals with similar peaks below 1 Hz are noticeable, but higher frequency components above 2 Hz are amplified, most likely due to the particular station location on the crest of the main crater (e.g., Ashford et al., 1997). A similar topographic effect is seen on records performed on the main rim in 2011 (see Fig. S1), thus excluding a potential signature of the intermittent activity of the new spatter cone. In the band [0.3–2] Hz, the frequency content of the seismic waveforms at Bulengo remarkably shows identical tremor patterns between 2011 and 2018, sometimes masked by hour-long perturbations most likely attributable into this frequency range to the microseisms from the nearby Lake Kivu (e.g., Xu et al., 2017). The analogy of the 2011 and 2018 seismic signals at Bulengo and Nyiragongo summit confirm that the lava lake generates a highly stable and persistent seismic tremor, even detectable at large distance. Because this seismic signal has an infrasonic counterpart (Barrière et al., 2018), the source process is connected to a shallow degassing mechanism, as discussed in the following section.

### 3.2. Seismically detected meter-scale variations of the lava lake level

Smets et al. (2017) attributed the minor variations of the lava lake level observed during the 2011 expedition to a gas piston effect due to gas trapping below the lake's crust, such as inferred at the multiple open vents of Kīlauea volcano for more than a century (e.g., Perret, 1913; Swanson et al., 1979; Patrick et al., 2016a). More specifically, observations at the Halema'uma'u lava lake are an important starting point for better understanding Nyiragongo



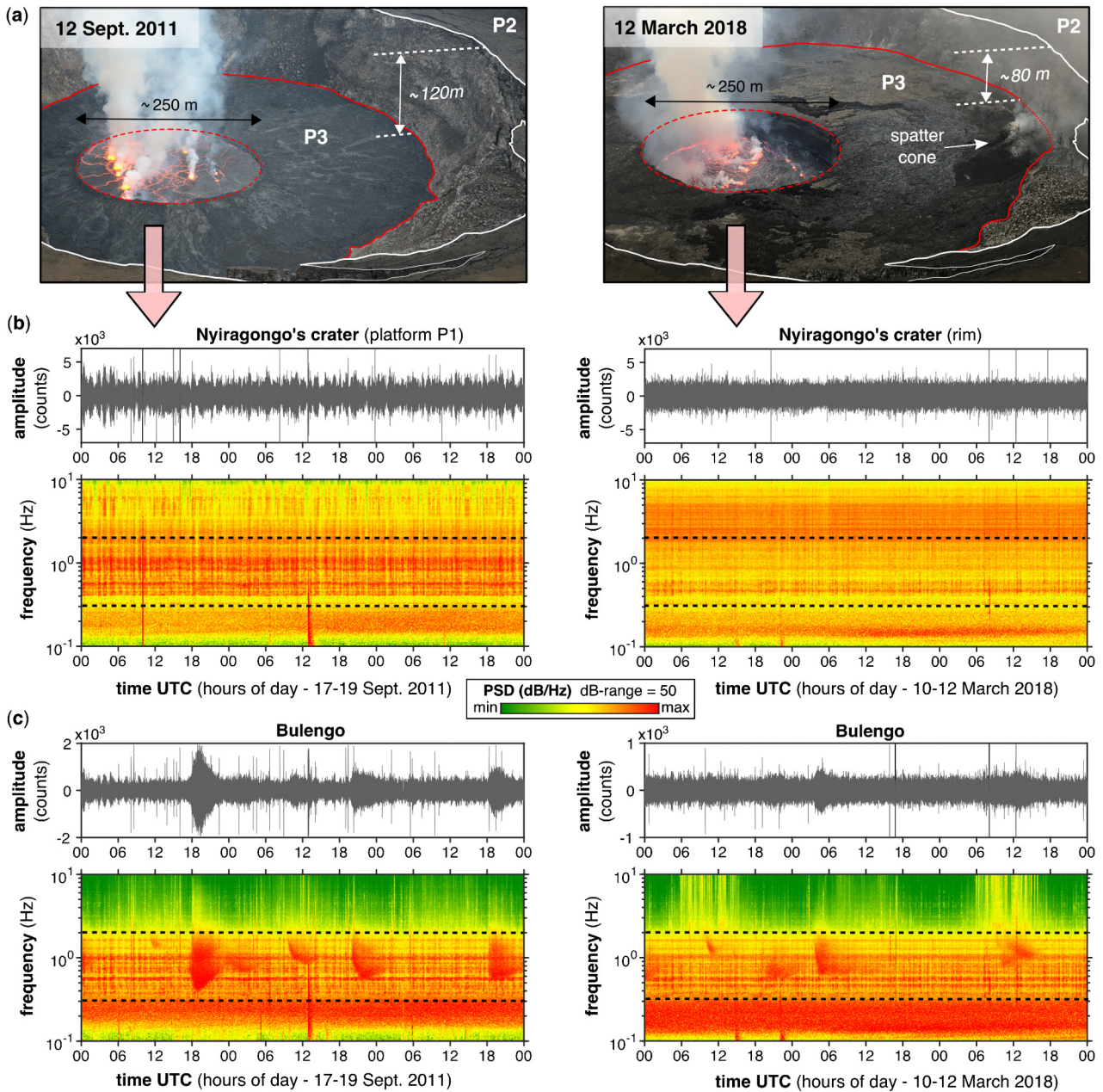


**Fig. 2.** – 2011 and 2018 – (a) Two pictures of Nyiragongo's lava lake spanning  $6^{1/2}$  yr (12 September 2011 and 12 March 2018), which were taken from the southern side of the rim (credit: B. Smets and N. d'Oreye). Approximate dimensions of the height of the platform P2 (with respect to P3) and the diameter of the lava lake are given. (b and c) Three days of seismic records at Nyiragongo's summit and Bulengo, respectively, during time periods associated to the pictures above (17–19 Sept. 2011 and 10–12 March 2018). The seismograms are raw waveforms (digital counts) filtered between 0.1 and 10 Hz and corresponding spectrograms into this frequency range are computed using the same parameters (50% overlapping Hamming window of 655-s length). The long-range continuous lava lake tremor signature is well detectable among all records between the dashed lines (frequencies ranging from approx. 0.3 to 2 Hz).

because of their similarity, be it in terms of lava viscosity, lake surface plate motions or lake dimensions (e.g., Patrick et al., 2016b; Valade et al., 2018). In addition to notable variations in infrasound records, degassing measurements and thermal imagery, Patrick et al. (2016a) showed that gas pistoning at Kilauea is likely due to a shallow gas trapping process also detectable by the amplitude modulation of the seismic tremor generated at the active vent. If such a phenomenon is applicable for Nyiragongo, then we should observe low tremor amplitude while the lake level rises and high amplitude tremor during periods of dominant spattering.

In order to detect amplitude variations of the lava lake seismic tremor, we calculate the root-mean-square (RMS) seismic amplitude filtered in the band [0.3–2] Hz using sliding 1-min windows overlapped every 6 s (i.e., 90% overlap). Fig. 3 shows the results

for 30 h on 18 and 19 September 2011 (Fig. 3a). The clear correlation between signals at Bulengo and Nyiragongo indicates that we can robustly characterize short-duration variations of the lava lake tremor over this large distance. The increases at Bulengo occurring at the end of each day during several hours correspond to local perturbations as explained previously for Fig. 2c (see section 3.1). The 3-h zoom window on 19 Sept. reveals long-term modulations of several tens of minutes to one hour. The apparent periodicity of these patterns is analyzed in the following section 3.3.

From almost two days of STLC recordings, Smets et al. (2017) were able to isolate six short sequences with sufficient visibility for estimating lake level variations (roughly 15 min to 1 h). Two out of these six time windows capture a significant and sudden increase of the lava lake level, and for one of these (on 19 Septem-

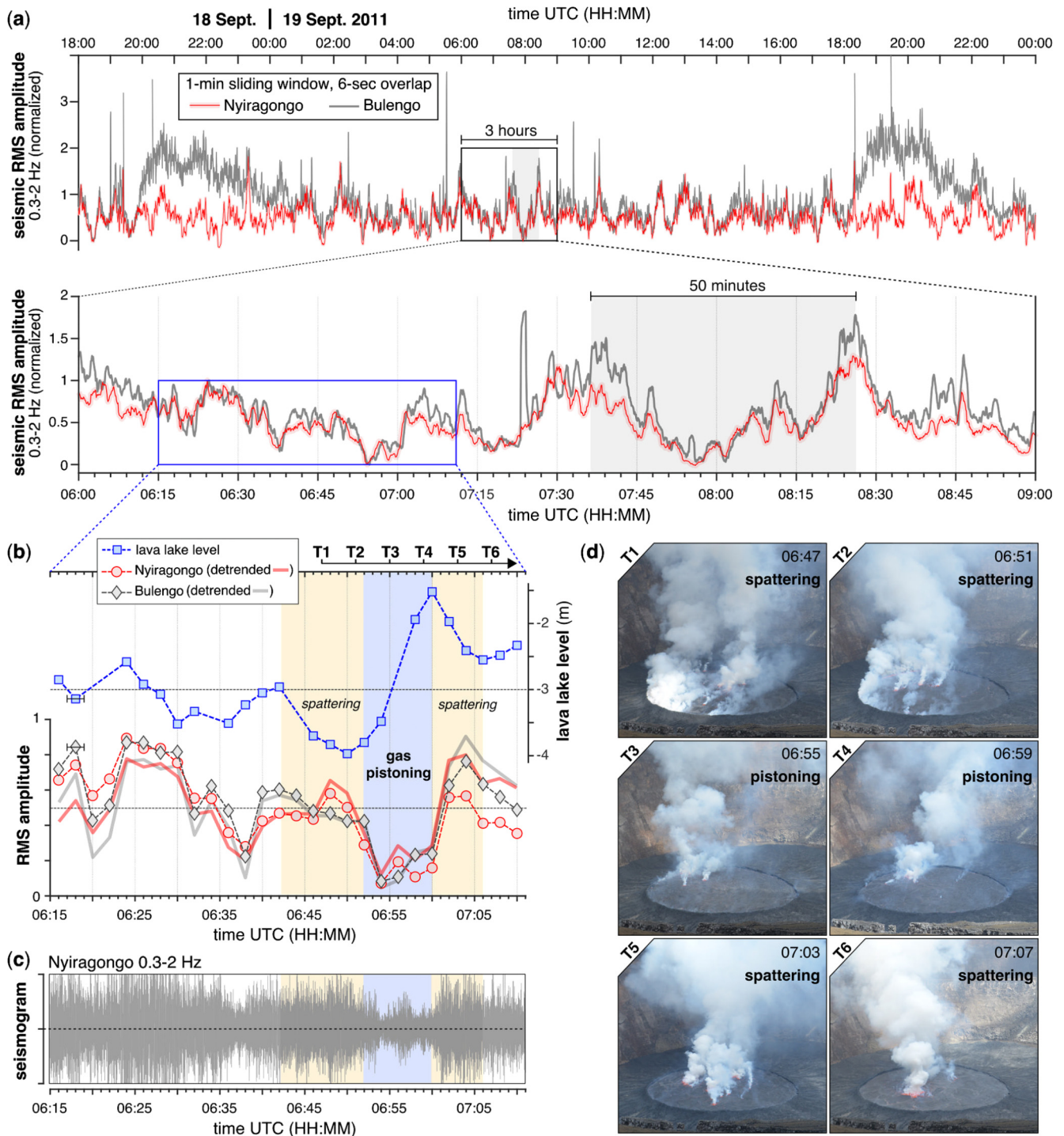


**Fig. 3.** – 2011 – (a) Sliding normalized RMS amplitude of vertical seismic records at Nyiragongo and Bulengo calculated using 6-sec overlapping windows of 1 min duration. Both curves are normalized with respect to the maximum and the minimum of the time period zoomed in (b), which is the single short-term period with available information about the lava lake level and simultaneous seismic records at Nyiragongo and Bulengo. Lava lake level variations are estimated from the STL images using the technique developed in Smets et al. (2017) with a standard error of about half a meter on average. RMS seismic amplitudes are downsampled to a similar sampling rate of 2 min (each point corresponds to the  $\pm 1$  min average of Fig. 3a) (round and diamond markers). A slightly better correlation with the lake level is obtained after removing the long-term trend (assumed to be linear), which seems independent of the level variations in this particular time window (thick solid lines). (c) The corresponding raw vertical seismogram at Nyiragongo’s summit is plotted for visual purpose (normalized units, clipped below and above the 1<sup>st</sup> and 99<sup>th</sup> percentiles respectively). (d) Six pictures corresponding to instants T1–T6 in (b), illustrating the transition from the spattering to gas pistoning regimes, and vice versa.

ber, Fig. 3b, c), simultaneous seismic measurements at Nyiragongo and Bulengo are available. As expected from a gas pistoning effect, the amplitude at both seismic stations decreases during phases of rising level and vice-versa. When the level rises by about 2.5 m in 8 min (between 06:52 and 07:00), the surface activity is markedly weaker (reduced spatter sources and thickness of the gas plume),

and the seismic amplitude decreases. This phenomenon is well illustrated by 6 consecutive images before, during and after this short-duration event (Fig. 3d).

The second time window with an apparent pistoning captured by Smets et al. (2017) occurred the following day on 20 September (Fig. 4). In this case, seismic records at Bulengo were useless due



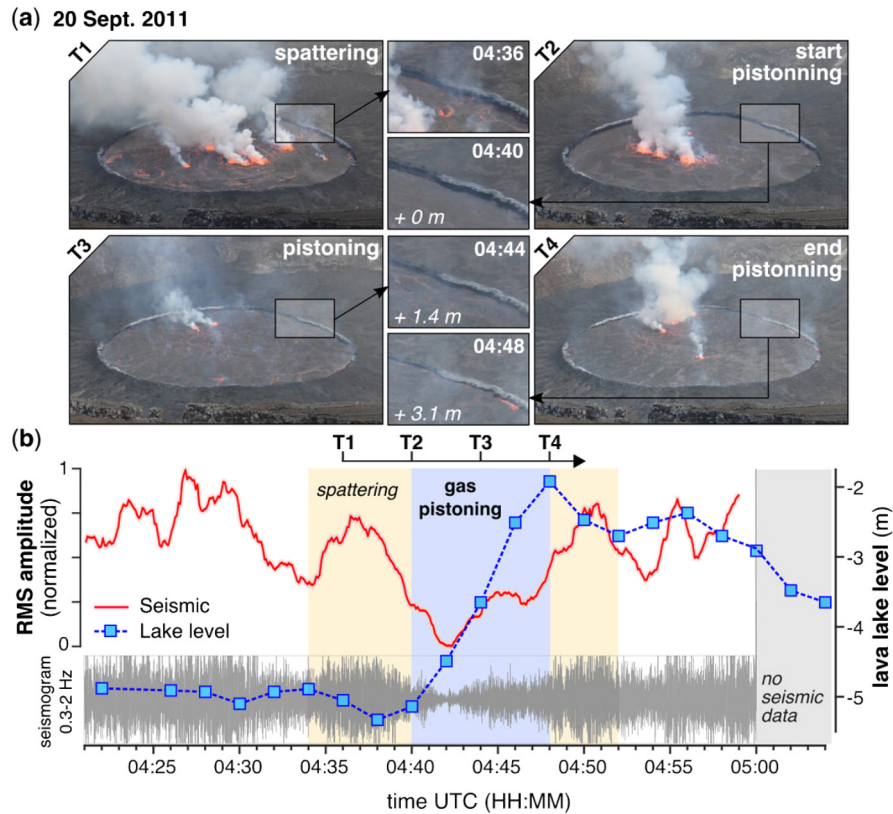


**Fig. 4.** – 2011 – (a) Four pictures (and associated zooms in the rim of the pit crater) with 4 min interval (T1–T4, 04:36 to 04:48) on 20 Sept. 2011 during a pistonning event. (b) Similarly to Fig. 3a, sliding normalized RMS amplitude using 6-s overlapping windows of 1 min duration (red line) of the vertical seismic records at Nyiragongo's crater. The corresponding seismogram is plotted in gray at the background, (normalized units, clipped below and above the 1st and 99th percentiles). The blue square markers correspond to the estimates of the lake level obtained by Smets et al. (2017).

to the many data gaps but the seismometer at the summit was only dismantled just after the rising phase of that pistonning event lasting again around 8 min. Alike in Fig. 3, Fig. 4a shows four pictures of the lava lake with additional zooms on the rim of the pit crater for visualizing the increase of the lake level by about 3 m. Fig. 4b shows that the main decrease of the seismic amplitude is once again attributable to the gas piston effect (see for instance picture T3 at 04:44 in Fig. 4a). The intensity, number and location of spatter sources most likely explain the high variability of the seismic amplitude at second/minute resolution.

### 3.3. Periodic patterns of the lava lake tremor

Beyond the short-term seismic amplitude variations reflecting the unsteady activity in the upper layer of the lake, the calculation of the 1-min sliding RMS amplitude provides indications for a more regular pattern of longer periods up to several tens of minutes (see Fig. 3a). In the framework of time-frequency (or equivalently time-period) analysis, a well-established method is the Continuous Wavelet Transform (CWT), which has been repeatedly used in volcanology, e.g., for studying the variations of the degassing patterns at Ambrym volcano (Allard et al., 2016) or the lava lake level at Halema'uma'u (Patrick et al., 2019).

Using the CWT, we aim to establish a representation of the dominant periods of the 1-min sliding RMS seismic amplitude, or in other words, the periodogram of the lava lake tremor. Our processing approach, which is detailed in the Supplementary Material (see Text S3 and Fig. S3), allows to construct a probability density plot of the global periodogram from local (instantaneous) estimates extracted from the wavelet transform. Fig. 5 shows such global periodograms obtained for 20 days between 5 and 24 March 2018 and for the 3 continuous days available in 2011 (17–19

September). In this latter case, the length of 3 days is too short for obtaining a robust probabilistic estimate and we directly plot the mean periodogram for the entire period (green line).

For the 2018 records, the mode of continuous maximum probability (black line) exhibits, both for Nyiragongo and Bulengo, a clear dominant periodicity  $T_D$  at around 25 min. In 2011, a dominant period is distinguishable at values two times greater than in 2018. Secondary components are also noticeable at shorter periods down to few minutes for both 2011 and 2018 records and correspond to intermittent and variable surface degassing processes (spattering and pistonning). For periods longer than about 120 min, no noticeable pattern stands out at Nyiragongo, while Bulengo is affected by strong and highly variable long-term components (e.g., Lake Kivu). Because similar shapes of periodograms are obtained at both locations (summit and Bulengo), the seismic amplitude variations up to periods of about 120 min reflect the (long-distance) lava lake tremor signature.

The dominant period  $T_D$  being well marked, we can easily track the variations of this peak value between March and November 2018 in order to better understand this particular property of the seismic tremor. Fig. 6a shows the continuous estimate of the dominant periodicity at Nyiragongo and Bulengo using sliding 20-days windows with 1-day overlap. The dominant period usually fluctuates around 20 min. However, early in September 2018,  $T_D$  suddenly increases up to 40–50 min. This longer periodicity lasting for about a month is associated with a decrease of the seismic amplitude in the frequency band [0.3–2] Hz (Fig. 6b). The simultaneous variations observed at the summit and at Bulengo confirm again that both recordings characterize a similar dominant source originating from the lava lake activity. This contrasts with the periodicity drop and amplitude increase observed only at Bulengo in July, conveying a seasonal effect due to the

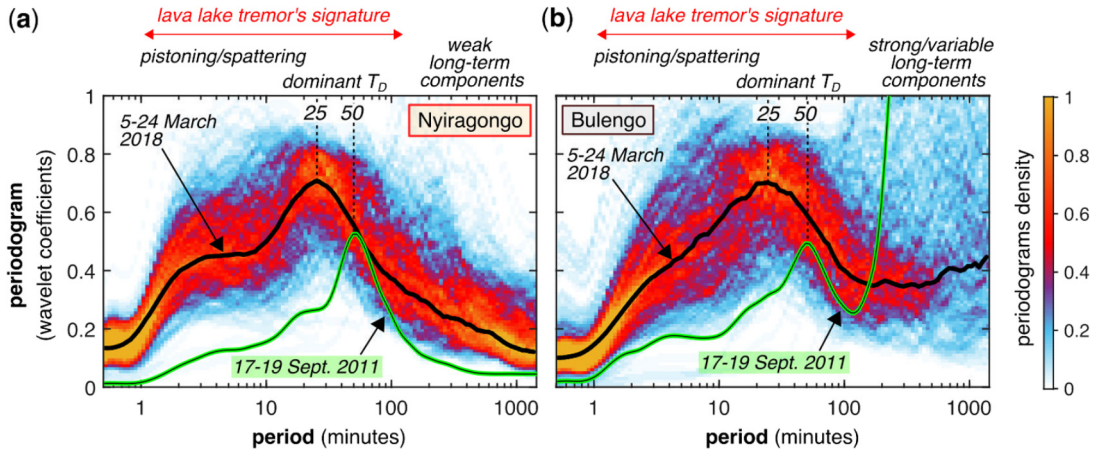


**Fig. 5.** – 2011 and 2018 – Periodograms of seismic amplitude variations for 20 days in March 2018 (probability density plot = blue-red-yellow color scale, maximum mode = black line) and for 3 days in September 2011 (mean periodogram = green line) obtained at (a) Nyiragongo and (b) Bulengo. The periodograms calculated from the CWT's wavelet coefficients are bounded between 0 and 1 in the range of periods [10–120] min due to necessary normalization procedures. A smoothing along the period axis is also performed, thus explaining why the maximum is significantly lower than 1 (see Supplementary Text S3 for more details). The sampling period of the RMS time-series (6 s) theoretically allows for the analysis of periods above 12 s (i.e., Nyquist period) but the chosen length of the averaging window (1 min) excludes the analysis of periods shorter than one minute, which are of little interest for the present study.

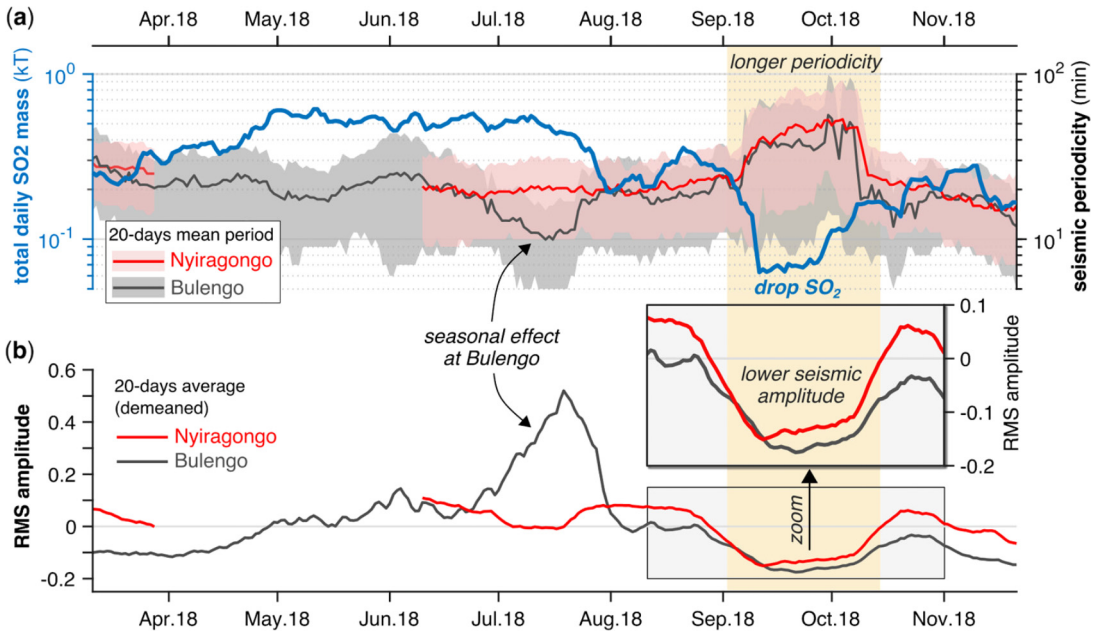


**Fig. 6.** – 2018 – (a) Total daily SO<sub>2</sub> mass (in kT, 20-days average) estimated with the TROPOMI sensor (left y-axis, blue) and the dominant seismic periodicity  $T_D$  of the lava lake (right y-axis) detected at the summit (red line) and at Bulengo (gray line) from overlapping 20-days periodograms (see Fig. 5). The corresponding shaded areas correspond to the 1-dB cutoff periods (i.e., the periods at which the periodogram amplitude is roughly higher than 0.9 times the maximum value).  $T_D$  corresponds to the mean value within the 1-dB range calculated as  $T_D = \frac{\sum(P * T)}{\sum T}$ , where T are the selected periods and P the periodogram values. All curves (SO<sub>2</sub>, seismic) are obtained for a similar computational window of  $\pm 10$  days overlapped by 1 day. (b) Amplitude of the same seismic time-series used for calculating the periodicity depicted in (a) (i.e., 1-min RMS values). Both curves for Nyiragongo and Bulengo are normalized over the entire period, averaged using windows of  $\pm 10$  days overlapped by 1 day, and finally demeaned for allowing a better comparison.

stronger amplitude of Lake Kivu's microseisms (see Fig. S4). In addition, we plot the space-based daily estimates of the total amount of SO<sub>2</sub> emissions originating from the lava lake on Fig. 6a (see section 2.3). Here, the most significant variation occurs early in September 2018 as well, as a sudden drop of degassing down to about one order of magnitude smaller than the maximum measured in May-July 2018 (i.e., 0.5 to 0.05 kT). The degassing remains at low level during a similar 1-month period, while the lava lake level remains unchanged (see Text S4 and Fig. S5). We interpret in the following section the close relationship between the variations of SO<sub>2</sub> and seismic tremor periodicity in terms of outgassing processes.

#### 4. Discussion: the outgassing mechanisms

In 1959, D. Shimozuru and E. Berg performed the first seismic measurements of Nyiragongo's lava lake activity and, to our knowledge, the only seismic dataset acquired at the summit crater reported in the literature. One of their main results is the detection of a periodic tremor signature of about 7 min comparable to our observations, even though we notice peak components at longer periods. This difference could be explained by the higher frequency band analyzed (the natural frequency of the geophone used is 4 Hz) and the substantially different configuration of the lava lake at that time. Sixty years later, this study remains one of

the best indications for the periodic nature of the lava lake activity, potentially linked to the dynamics of the shallow reservoir as suggested by these authors. In the following, we discuss new insights confirming this statement.

#### 4.1. Intermittent shallow-rooted pistoning of the lava lake

The coupled seismic and lake level measurements performed at the summit of Nyiragongo (see Figs. 3, 4 and section 3.2) provide highly valuable insights into the shallow-rooted degassing mechanisms of its lava lake system. In analogy with the Halema'uma'u lava lake in Hawaii, the short-term amplitude variations of the seismic tremor (see also Fig. 5 and section 3.3), correlated to meter-scale level variations, validate the model of temporary gas trapping in the upper layer of the lake and its subsequent release. Conversely, a typical day at Halema'uma'u is characterized by a very sharp transition of the tremor amplitude between long-duration (few hours) "stable non-spattering" and "unstable spattering" (Patrick et al., 2016b). Patrick et al. (2016a) observed pistoning of a few to 20 m at Kilauea. This phenomenon probably cannot develop in such a large extent (smoother and short-duration variations with peak-to-peak level differences of about 2.5 and 3.1 m) because of the particular size and dynamics of Nyiragongo's lava lake. The fast motion of the crust often exceeding 0.1 to 1 m s<sup>-1</sup> (Sawyer et al., 2008; Valade et al., 2018) might hamper the formation of a homogeneous upper layer acting as a sustained barrier to degassing. More continuous observations at the summit are needed in order to potentially detect larger pistoning events. For instance, Burgi et al. (2014) observe some sudden rises of the lake level of a few meters during four days in June 2010 referred as due to "undetermined degassing conditions".

#### 4.2. Continuous deeply-sourced lava lake convection

At this point it is important to differentiate the two distinct signatures of the lava lake tremor generated in the same near-surface source region. As described above (section 4.1), its short-term signature (seconds to minutes) originates from the surface spattering/pistoning activity and is highly variable. On the other hand, the dominant periodic peaks ( $T_D = 50$  min in 2011,  $T_D = 25$  min in 2018) could be a signature of a periodic convective movement of the lava lake and, in turn, potentially linked to the degassing regime of a shallow magma chamber. We first investigate some potential models of degassing at Nyiragongo explaining the gas measurements performed at the summit by Sawyer et al. (2008) and then propose an interpretation based on our seismic observations.

Petrological investigations by Demant et al. (1994) and Platz et al. (2004) constrain the location of the feeding shallow reservoir at a depth of 1 to 4 km, connected to the lava lake by a conduit of unknown dimensions. Within this range of depths, two major gas species (CO<sub>2</sub> and SO<sub>2</sub>) escape from the magma due to the decreasing pressure, but do not exsolve at the same depth (shallower for SO<sub>2</sub>). The stable ratio of CO<sub>2</sub> to SO<sub>2</sub> measured between 2005 and 2007 by Sawyer et al. (2008) indicates a continuous equilibrium between the two gas phases while the ascending magma rises in the feeding conduit. In other words, a model of a gas slug periodically moving upwards from the magma reservoir (e.g., collapse foam model by Jaupart and Vergnolle, 1989) is unlikely because, in this situation, the difference of solubility between CO<sub>2</sub> and SO<sub>2</sub> should be noticeable at the surface.

Sawyer et al. (2008) propose the Rise Speed Dependent (RSD) model (Parfitt and Wilson, 1995) as more appropriate for describing the degassing at Nyiragongo. This way, the stable CO<sub>2</sub>/SO<sub>2</sub> ratio is explained by the continuous, hierarchic exsolution of volatiles traveling at a similar speed to the lava lake. Moreover, because the

magma influx must be high in order to maintain a molten state in the lake (0.6 to 3.5 m<sup>3</sup> s<sup>-1</sup> according to Burgi et al., 2014), the mechanism at Nyiragongo may consist of a relatively homogeneous two-phase flow of high speed (>0.1 m/s) as inferred for Hawaiian eruptions (Parfitt and Wilson, 1995). A steady-state degassing driving the lake convection well explains the persistent and stable nature of the lava lake tremor, yet the mechanisms behind the fluctuating periodicity of this convection pattern as inferred from the shallow seismicity (Fig. 6) remain unclear.

Similarly to the 2005–2007 measurements by Sawyer et al. (2008), Le Guern (1987) observed constant ratios between the primary volatile elements H<sub>2</sub>O, CO<sub>2</sub> and SO<sub>2</sub> between 1959 and 1972. We can thus reasonably assume that the fluctuation of SO<sub>2</sub> emissions in September 2018 is a proxy for overall degassing conditions (Fig. 6a), where H<sub>2</sub>O is the most abundant gas as it is usually observed within basaltic magmas (Sawyer et al., 2008). Being the driving force of the magma movement, the decrease of the gas influx intuitively explains a reduction in speed of the convection within the lava lake inferred from the longer periodicity (Fig. 6a) and lower amplitude (Fig. 6b) of the associated tremor. This observation thus highlights a noteworthy result of our study: If generated by the convective movement within the lava lake, the dominant periodic signature of the surface seismic tremor could be linked to the degassing regime of the shallow magma chamber. However, an important question remains: how can the seismic tremor generated close to the lake surface be connected to this convective mechanism and, as a result, how deep would the dominant convective cell be?

In accordance with Sawyer et al. (2008), we propose a simple convective process dominantly driven by magma buoyancy but also accounting for the effect of thermal convection (e.g., Worster et al., 1993). At Nyiragongo, Le Guern (1987) pointed out the importance of heat transfer at the top of the lake as a probable cause of superficial convection (i.e., cooling process), while the lava lake activity is maintained by the gas expansion. Ascending hot gas-rich magma progressively accumulates and degases continuously at the surface through the lake's crust *via* the spattering activity or is intermittently trapped within a foamy head at the top of the lake (i.e., pistoning), thus leading to minor increases of the lake level. After some critical mass is reached, a denser and cooler slug of magma sinks back down into the conduit. As a result, the regular replenishment of this near-surface layer can induce long-term, quasi-periodic variations of the seismic tremor intensity.

In light of these findings, we propose a conceptual model of the lava lake dynamics controlled by competitive shallow and deep outgassing processes, as illustrated in Fig. 7. Considering the only very recent multi-disciplinary observation of the lava lake (i.e., SO<sub>2</sub> from TROPOMI and summit seismic measurements since early 2018), it is not yet possible to discuss a potential link between the fluctuations of the lake level and the temporal variation of this convective process. We can, however, already note that the 1-month event of September 2018 (see Fig. 6) is not associated with any clear drop of the lake, maintaining its level close to the platform P3 at that time (see Text S4 and Fig. S5). We present below a totally different mechanism in order to explain the majors drops of the lava lake already reported in the literature.

#### 4.3. Deep intrusion-related degassing events

The conceptual model of the lava lake outgassing proposed here (Fig. 7) implies a stable gas composition over the last decades in accordance with measurements reported by Sawyer et al. (2008) and Le Guern (1987). Short-term changing gas compositions can however occur as observed by Bobrowski et al. (2017) from several individual measurements between 2007 and 2011. In particular during a single campaign in June 2011, they detected a significant



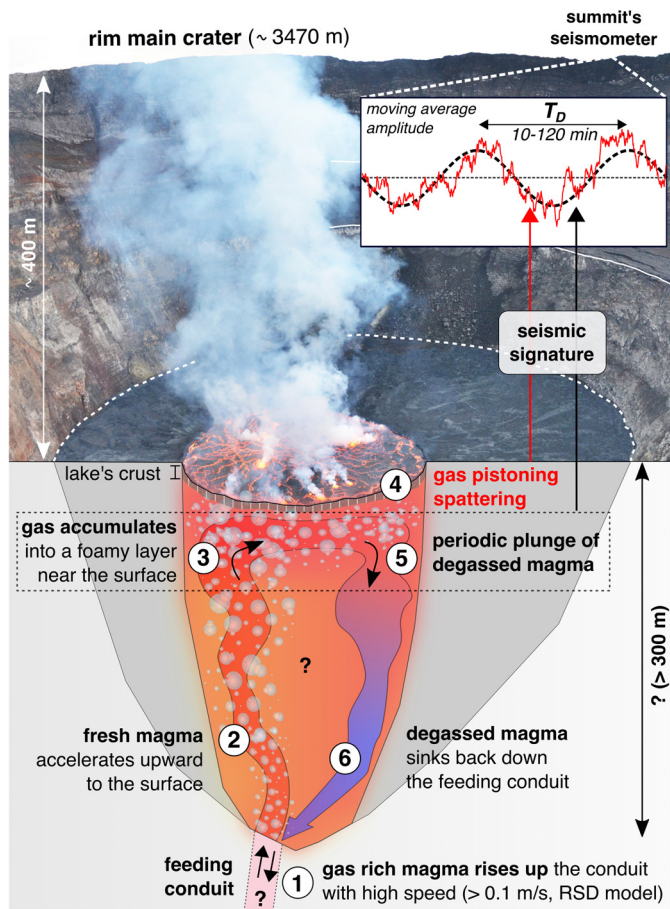


**Fig. 7.** Conceptual model of convection and degassing mechanisms of the Nyiragongo lava lake system inferred from close-range seismic observations and space-based  $\text{SO}_2$  estimates (steps 1 to 6, see text for more details). RSD model stands for “Rise Speed Dependent” (e.g., Parfitt, 2004). The background image is part of a panoramic picture taken by B. Smets during the 2011 expedition. For illustrative purpose, the seismometer is located on the northern part of the rim but the instrument has actually been deployed on the southern side in 2011 and 2018 (see Fig. 1b). The depth of the lava lake is estimated to be larger than 300 m since 2011 as inferred from observations of the crater morphology after the collapses of the crater in 1977 and 2002 (see text S6).

increase of  $\text{SO}_2$  and Cl after a major decrease of the lava lake level on 3 June (estimated around 25 m), followed up by a more intense surface activity. Bobrowski et al. (2017) or similarly Burgi et al. (2014) explain the lowering of the lake during this specific episode through the displacement of gas as the cause of the pressure drop. However, this hypothesis suffers from the lack of other observations while the analysis of available seismic records at that time suggest that such pressure drop is actually induced by magma intrusion at large depth.

Using seismic and infrasound data recorded at the foot of the volcano, Barrière et al. (2018) characterized a similar sudden major drop of the lava lake level ( $\sim 80$  m) in November 2016 associated with a seismic swarm. Barrière et al. (2018) show that this phenomenon is most likely a coupled process of deep magma intrusion (at least deeper than 5 km b.s.l.) and partial drainage of the lava lake as repeatedly observed at the Halema’uma’u crater in Hawaii (Patrick et al., 2015). The analysis of available seismic data from Bulengo station also reveals a similar seismic swarm occurring in the evening of 3 June 2011, corresponding to the timing of the lava lake drop reported by Bobrowski et al. (2017). The beginning of the 2011 and 2016 swarms (4-h seismic records at Bulengo) and pictures of the lava lake taken several weeks after both magmatic intrusions are displayed in Fig. 8. These seismic swarms,

both ending early the next morning, are constituted by events having some characteristics of volcano-tectonic earthquakes (i.e., high-frequency onset) but also pronounced low-frequency wave trains (see Fig. S6). Battaglia et al. (2003) locate similar deep “hybrid” events (classified as Long-Period – LP) beneath Kilauea at around 5 km b.s.l. and suggest the source of the precursory high-frequency onsets as due to the fracturing of the rock by the pressurized magma. While we cannot determine the focal depths in June 2011 (too few stations), the source region in November 2016 could be obtained thanks to the KivuSNet stations. The chosen approach is detailed in the Supplementary material (see Text S5 and Figs. S7–S11), while a brief summary and the main results are presented below (Figs. 8 and 9).

Since the second phase of deployment of KivuSNet (Sept–Oct. 2015, see Oth et al., 2017), a batch of low-amplitude seismic events has been located below Nyiragongo at more than 10 km depth (e.g., Barrière et al., 2018). These events have a pronounced high-frequency signature (i.e.,  $> 5$  Hz) at most of the stations, with characteristics of traditional (tectonic) earthquakes with clear onset for the most energetic events. This cluster is actually constituted by highly similar events (see Supplementary Fig. S8), which would logically suggest a stable and non-destructive source. Such kind of highly repetitive events at volcanoes are generally characterized by lower frequency content (i.e., LP-type) but fluid-related movements within a particular deep storage or feeding zone might be responsible for such higher frequency excitation (e.g., Caplan-Auerbach and Petersen, 2005). We use this particular property of repetitiveness in order to obtain a single accurate location of a master (or reference) event build from the stack of more than 5000 nearly identical events detected between September 2015 and 2018. We obtained a first guess for the absolute location estimates of the November 2016 swarm events relative to this reference event using a standard “master event (ME)” location technique (e.g., Evernden, 1969). The final location solutions are then refined for a set of selected swarm earthquakes satisfying quality criteria (e.g., sufficient number of observations/stations) by minimizing the relative errors between events using a double-difference (DD) algorithm (Waldhauser and Ellsworth, 2000). Details about both complementary location methods are given in the Supplementary material (Text S5 and Figs. S7–S11).

These swarm events (Fig. 9) are located mostly between 11 to 14 km b.s.l. beneath the volcanic edifice and can be related to the probable presence of a deep reservoir at around 10–14 km inferred from petrological investigations (Demant et al., 1994). The depth range of the swarm events seems broader at the beginning and then decreases with time into a more concentrated cluster. This pattern potentially reflects the seismic activity at the base of a lateral opening dyke such as observed in Iceland during the 2014–15 Bárðarbunga rifting event (Woods et al., 2018). More interestingly, the beginning of the swarm indicates the start of the magmatic intrusion close to the master – repetitive – event (represented in Fig. 9 by its 68% confidence ellipsoid). Its progression during the next hours follows a direction SW–NE. This orientation corresponds to the direction of the principal rift faults of the Precambrian basement in the VVP indicating some preferential structure weaknesses for magma intrusion at depth (Smets et al., 2016). More detailed investigations about this swarm and other potential intrusions associated with lava lake drops as well as a dedicated analysis of the source mechanism of the repetitive (master) events will be the subject of future studies.

In summary, both 2011 and 2016 sequences thus initiated with a seismic swarm synchronous with the drop of the lava lake, followed by strong degassing and surface activity of the lava lake as evidenced from abnormally high infrasound levels and near-surface low-frequency seismicity in November 2016 (Barrière et al., 2018) or direct gas measurements and visual observations in

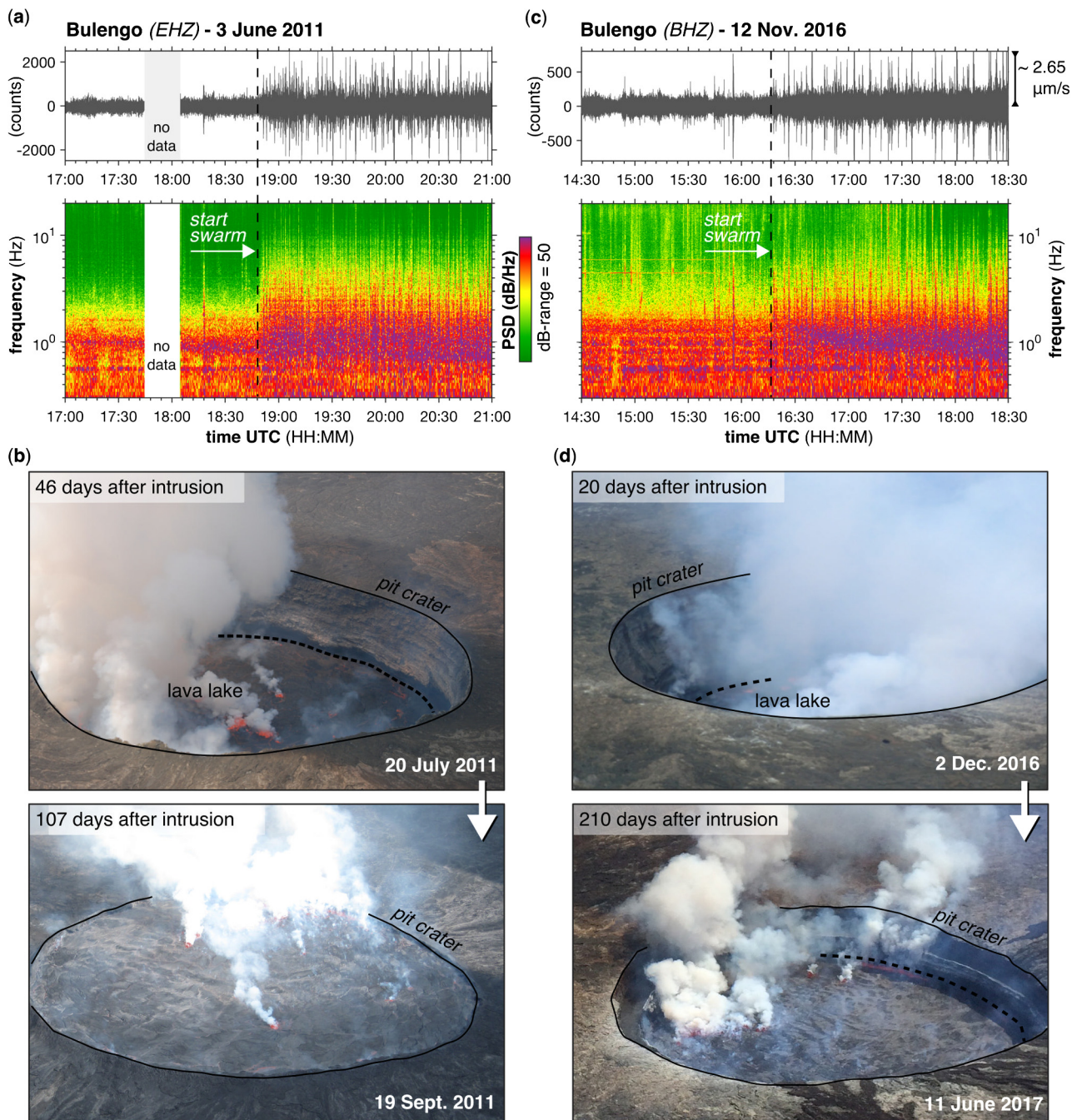


**Fig. 8.** – 2011 and 2016/2017 – (a) 4-h seismogram and corresponding spectrogram at Bulengo on 3 June 2011. Units are digital counts and traces are high-pass filtered above 0.3 Hz. (b) Two pictures of Nyiragongo's lava lake several weeks after the swarm (and associated drop of the lava lake level) taken from the southern side. These pictures illustrate the progressive pressure build-up (increasing lava lake level) after the magmatic intrusion. (c) and (d) Same as (a) and (b) for the swarm starting on 12 November 2016. Knowing the instrumental response in 2016, the scale in  $\mu\text{m/s}$  after applying linear gain correction is also indicated. For the seismograms, BHZ and EHZ means broadband and short-period vertical component records, respectively. The photos taken on 2 Dec. 2016 and 20 July 2011 are courtesy of GVO and Antoine Kies, respectively. The lake depth is estimated to be  $\sim 100$  m below the rim of the pit crater in Dec. 2016, and  $\sim 50$  m in July 2011.

June 2011 (Burgi et al., 2014; Bobrowski et al., 2017). While it remains unclear how these intrusions modify the dynamics of the magmatic system, such major pressure drops can disrupt the steady behavior of the lava lake and induce more or less persistent changes at depth by modifying properties of the depleted magma sources. Rockfalls from the walls of the pit crater destabilized by the drop of the lake can also occur and participate to the agitated surface activity and strong degassing (e.g., Patrick et al., 2016b). Both in 2011 and 2016, the lava lake continued to decrease progressively after the events (Burgi et al., 2014; Barrière et al., 2018) and maintained at low level several weeks

after the main drops (up to  $\sim 50$  m and  $\sim 100$  m below the rim of the pit crater in 2011 and 2018 respectively). It returned to the level of platform P3 several months later as a consequence of the progressive pressure build-up within the plumbing system (see Fig. 8b).

##### 5. Deciphering the lake dynamics from its surface motion?

According to the conceptual model proposed here (Fig. 7), time-varying properties of surface observations, e.g., number and location of spatter sources, motions, size and temperature of the



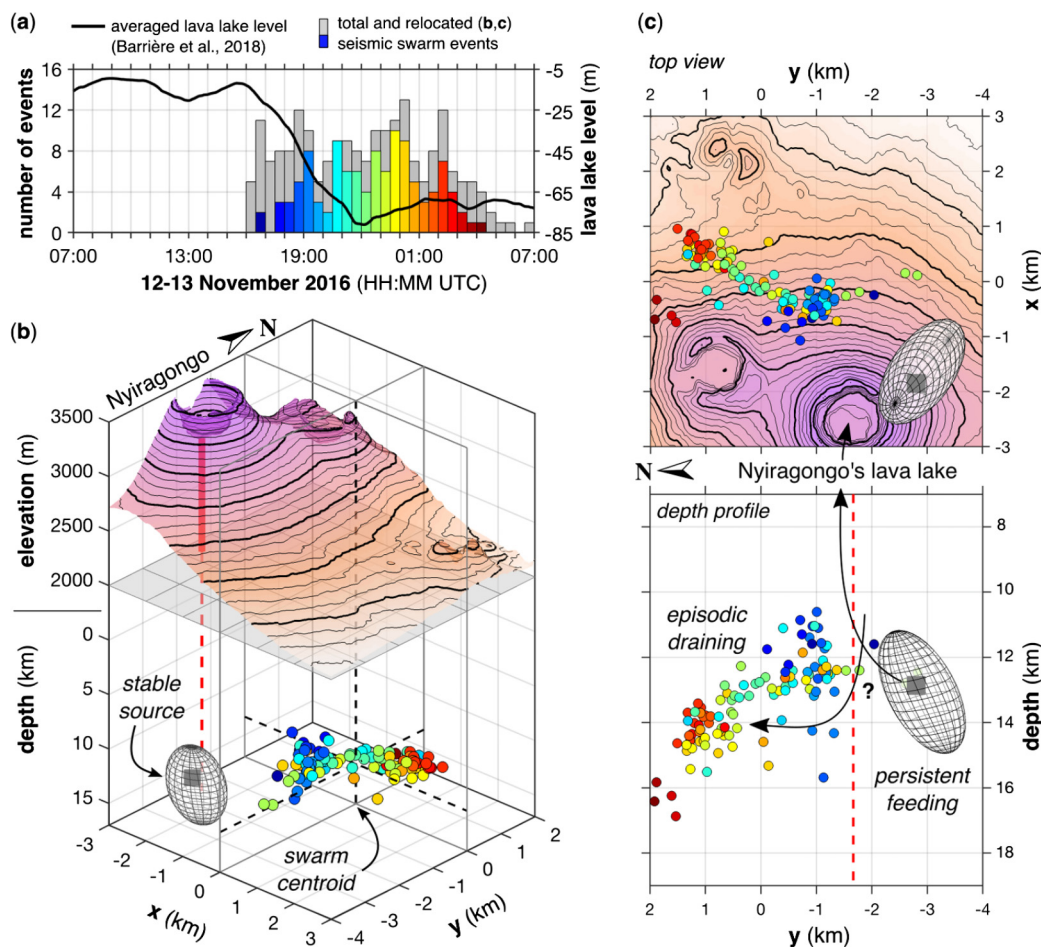


**Fig. 9.** – 2016 – (a) Number of events and lava lake level during the November 2016 swarm. Gray histogram corresponds to the total number of events detected beneath Nyiragongo and colored histogram correspond to events that can be adequately located. Each color is associated to a 30-min window. (b) 3D view of hypocenters of the swarm and master events, the latter being represented by its maximum likelihood – square gray marker – and its 68% confidence ellipsoid assuming errors following Gaussian distribution. Please see the Supplementary Text S5 for more details about the location procedure. (c) Top view and depth profile from (b) illustrating the persistent feeding of the lava lake probably associated to the master event and its episodic draining that occur as the result of a magmatic intrusion associated with the seismic swarm. Considering a lava density of  $2.5 \cdot 10^3 \text{ kg/m}^3$  and neglecting the frictional pressure loss in the conduit, a lake level drop by 80 m such as the one observed in November 2016 corresponds to a magma-static pressure drop of about 2 MPa, the same order of magnitude as the overpressure within the 2002 eruptive dikes estimated by Wauthier et al. (2012).

plates, could be connected to the lake convection. In a recent study combining surface observations for different lava lakes, Lev et al. (2019) propose two classes of lava lakes following the global relationship between lake size, lake surface motion and total gas flux. Nyiragongo is classified (with Kilauea after 2011 and Erta’Ale) as “organized lake” with few modes of surface motion in contrast to “chaotic ones” (Villarica, Masaya, Marum), while Erebus would belong to both types. In both cases, the convective process is mainly controlled by the upwelling of fresh and gas-rich magma that accumulates and degases at the surface as proposed in the present study. Lev et al. (2019) notably conclude their study by indicating that surface motion could bring additional information regarding the lake convection through three main types of plate movements. “Radial” or “multi-radial” motions, which correspond to one or multiple upwelling regions in the interior and downwelling zones along the edges, would indicate a bi-directional flow between upwelling and downwelling material. The third case (“side-to-side”) would be due to a lower viscosity contrast between the ascending and downgoing flows resulting in a more stable side-to-side surface motion. The dominant motion pattern from a sustained upwelling area close to the rim of Halema’uma’u lava lake (e.g., Patrick et al., 2016b) is classified in this third category.

Based on thermal images collected by Spampinato et al. (2013) in March 2012, Lev et al. (2019) assume the surface motion at Nyi-

ragongo as dominantly radial (from the western part of the lake), even though noticeable spatial variations of plate divergence and convergence are also observed. From another thermal imaging survey performed in April 2016 at Nyiragongo, Valade et al. (2018) propose a convective model with a dominant upwelling in the central region of the lake and downwelling movements at some parts of the rim accompanied by spattering and degassing. This model is obtained by averaging temperature and velocity gradients over few hours in order to remove the complex short-term surface motion of “multi-radial” type (i.e., multiple upwelling and downwelling areas). In contrast to such radial behavior, a near-infrared imaging survey in June 2017 that we report here for the first time reveals a clear long-lasting upwelling area close to the northern rim of the pit crater (see Supplementary Video S1). This particular motion thus potentially reflects a different outgassing regime of type “side-to-side” such as observed at Kilauea.

A more detailed analysis remains beyond the scope of this paper but this preliminary investigation already indicates that Nyiragongo exhibits more types of surface plates motion than Lev et al. (2019) attribute to this volcano based on the single study by Spampinato et al. (2013), thus complexifying the interpretation of the deep circulation from the surface movements. In contrast to the case of Halema’uma’u, where the transition from chaotic in 2009 to organized and dominant “side-to-side” motion since 2011



can be reasonably explained by a change in lake size (Lev et al., 2019; Patrick et al., 2016a), the dimensions (height, width) of the Nyiragongo lava lake are roughly the same during these three expeditions and, consequently, should not play a major role on the observed surface motions. This variability might therefore rather reflect the changing properties (e.g., bubble sizes, gas content, temperature) of the ascending magma from the shallow reservoir (Lev et al., 2019). A totally different explanation of the agitated surface motions observed by Spampinato et al. (2013) or Valade et al. (2018) would be the phenomenon of superficial “spattering-driven flow” described by Patrick et al. (2016b) at Halema’uma’u. In this unsteady situation, the surface motion is controlled by surface depression consecutive to bubbles bursting and hence does not convey any information about the convective movements. In this case, only the sustained and placid “side-to-side” pattern observed in June 2017 (Video S1) could be considered as a proxy of the lake convection, the upwelling area being consistently located at the north of the lake where the main conduit outlet has already been reported by old visual observations (i.e., fountaining) about 800 m below the crater rim after collapses of inner platforms (e.g., Durieux, 2002; Tazieff, 1984). As exemplified at Kilauea (Patrick et al., 2016b), more long-term multi-disciplinary observations at the summit remain essential to better understand the link between the dynamics of the lava lake system and its surface behavior.

## 6. Conclusion

Three important magmatic processes at Nyiragongo related to its lava lake activity are deciphered from the analysis of shallow (tremor) and deep (swarm) seismicity:

- **Continuous gas pistoning and spattering:** Small meter-scale lava lake level variations are seismically detected at long distance and correspond to a shallow degassing mechanism similar to the one inferred at the Halema’uma’u lava lake (i.e., gas pistoning and spattering). The pistoning episodes observed in September 2011 did not exceed 10 min.
- **Periodic lake convection:** The dominant periodicity of the lava lake tremor tends to fluctuate between around 10 min to one hour in accordance with the long-term variations of SO<sub>2</sub> degassing. This pattern is thus interpreted as a proxy of the main convective movement and depends of the time-varying properties of the ascending gas-melt mixture from the shallow magma chamber. A potential link with fluctuations of the lake level has not been observed yet.
- **Transient large lake level drops with strong degassing:** Major sudden decreases of the lake level such as reported by Bobrowski et al. (2017) and Burgi et al. (2014) in June 2011 or Barrière et al. (2018) in November 2016 are well explained by a pressure drop within the magmatic system due to deep magma intrusions.

The multi-disciplinary datasets gathered here lead to a comprehensive conceptual model unraveling the outgassing dynamics at a lava lake system. Analyzing changes in seismic tremor amplitudes allows for a consistent description of superficial manifestations (pistoning, spattering). The periodic signature of the gas-driven convective mechanism within the lake is also contained in the tremor signal, while the analysis of surface plates motion alone provides more ambiguous information. This study thus highlights the benefits of monitoring the ambient seismic signal generated by lava lake activity in order to potentially connect surface processes with changing properties of the ascending gas-rich magma. Having a complete view of the underlying mechanisms responsible for major changes of lava lake activity also implies the analysis of magma movements at the level of deeper magma storage. Thanks

to the identification of deep seismic swarms (>10 km b.s.l.), sudden large drops of the lava lake level associated with a strong degassing are explained by major pressure changes in the magmatic reservoir due to lateral dyke intrusion at large depths.

## Acknowledgements

We thank M. Patrick and an anonymous reviewer for their constructive reviews and the editor T. Mather for her comments, which help to improve the original manuscript. This article is a contribution in the framework of the following projects: “Remote Sensing and In Situ Detection and Tracking of Geohazards” (RESIST, <http://resist.africamuseum.be>), funded by the Belgian Science Policy Office (Belspo), Belgium, and the Fonds National de la Recherche (FNR), Luxembourg, and “Split band assisted Multi-dimensional and Multi-zonal InSAR time series Processor” (SMMIP) funded by the Fonds National de la Recherche (FNR), Luxembourg. We also wish to thank the Congolese Institute for Nature Preservation (ICCN) and the MONUSCO for their continuous support and for allowing us to host the stations in their compounds, as well as the entire Goma Volcano Observatory team and the sentinels of the stations, without whom the operation of the seismic network would be impossible. KivuSNet data are underlying an embargo policy following the conditions of the Memoranda of Understanding between the partner institutions of RESIST. Beyond this embargo policy, data may be shared for collaboration purposes upon request with the approval of all involved RESIST partners. Data archiving and accessibility is ensured through the GEOFON program of the GFZ German Research Centre for Geosciences (<https://doi.org/10.14470/XI058335>) and KivuSNet is registered within the FDSN with network code KV (<http://www.fdsn.org/networks/detail/KV/>). The work related to TROPOMI SO<sub>2</sub> data has been performed in the frame of the TROPOMI project. We acknowledge financial support from the European Space Agency (ESA) S5P and Belgium Prodex TRACE-SSP projects. Sentinel 1 SAR images (Supplementary information, Fig. S5) are provided by ESA.

## Appendix A. Supplementary material

Supplementary material related to this article can be found online at <https://doi.org/10.1016/j.epsl.2019.115821>.

## References

- Allard, P., Burton, M., Sawyer, G., Bani, P., 2016. Degassing dynamics of basaltic lava lake at a top-ranking volatile emitter: Ambrym volcano, Vanuatu arc. *Earth Planet. Sci. Lett.* 448, 69–80. <https://doi.org/10.1016/j.epsl.2016.05.014>.
- Ashford, S.A., Lysmer, J., Sitar, N., Deng, N., 1997. Topographic effects on the seismic response of steep slopes. *Bull. Seismol. Soc. Am.* 87, 701–709.
- Barrière, J., Oreye, N., Oth, A., Geirsson, H., Mashagiro, N., Johnson, J.B., Smets, B., Samsonov, S., Kervyn, F., 2018. Single-station seismo-acoustic monitoring of Nyiragongo’s lava lake activity, D.R. Congo. *Front. Earth Sci.* 6. <https://doi.org/10.3389/feart.2018.00082>.
- Barrière, J., Oth, A., Theys, N., d’Oreye, N., Kervyn, F., 2017. Long-term monitoring of long-period seismicity and space-based SO<sub>2</sub> observations at African lava lake volcanoes, Nyiragongo and Nyamulagira (DR Congo). *Geophys. Res. Lett.* 44, 6020–6029. <https://doi.org/10.1002/2017GL073348>.
- Battaglia, J., Got, J.-L., Okubo, P., 2003. Location of long-period events below Kilauea Volcano using seismic amplitudes and accurate relative relocation. *J. Geophys. Res.* 108, 2553. <https://doi.org/10.1029/2003JB002517>.
- Bobrowski, N., Giuffrida, G.B., Yalire, M., Lübcke, P., Arellano, S., Balagizi, C., Calabrese, S., Galle, B., Tedesco, D., 2017. Multi-component gas emission measurements of the active lava lake of Nyiragongo, DR Congo. *J. Afr. Earth Sci.* 134, 856–865. <https://doi.org/10.1016/j.jafrearsci.2016.07.010>.
- Bobrowski, N., von Glasow, R., Giuffrida, G.B., Tedesco, D., Aiuppa, A., Yalire, M., Arellano, S., Johansson, M., Galle, B., 2016. Gas emission strength and evolution of the molar ratio of BrO/SO<sub>2</sub> in the plume of Nyiragongo in comparison to Etna. *J. Geophys. Res.* 120, 277–291. <https://doi.org/10.1002/2013JD021069>.
- Burgi, P.-Y., Darrach, T.H., Tedesco, D., Eymold, W.K., 2014. Dynamics of the Mount Nyiragongo lava lake. *J. Geophys. Res., Solid Earth* 119, 4106–4122. <https://doi.org/10.1002/2013JB010895>.

- Caplan-Auerbach, J., Petersen, T., 2005. Repeating coupled earthquakes at Shishaldin Volcano, Alaska. *J. Volcanol. Geotherm. Res.* 145, 151–172. <https://doi.org/10.1016/j.jvolgeores.2005.01.011>.
- Chouet, B., Dawson, P., 2015. Seismic source dynamics of gas-piston activity at Kilauea Volcano, Hawaii. *J. Geophys. Res., Solid Earth* 120, 2525–2560. <https://doi.org/10.1002/2014JB011789>. Received.
- de Magnée, I., 1959. Première exploration géophysique du volcan Nyiragongo (Kivu). *Bull. Séances Acad. R. Sci.* 2, 379–401.
- Demant, A., Lestrade, P., Lubala, R.T., Kampunzu, A.B., Durieux, J., 1994. Volcanological and petrological evolution of Nyiragongo volcano, Virunga volcanic field, Zaire. *Bull. Volcanol.* 56, 47–61. <https://doi.org/10.1007/BF00279728>.
- Durieux, J., 2002. Volcano Nyiragongo (D.R. Congo): evolution of the crater lava lakes from the discovery to the present. *Acta Vulcanol.* 14–15, 137–144.
- Evernden, J.F., 1969. Identification of earthquakes and explosions by use of teleseismic data. *J. Geophys. Res.* 74, 3828–3856. <https://doi.org/10.1029/JB074i015p03828>.
- Hamaguchi, H., Nishimura, T., Zana, N., 1992. Process of the 1977 Nyiragongo eruption inferred from the analysis of long-period earthquakes and volcanic tremors. *Tectonophysics* 209, 241–254. [https://doi.org/10.1016/0040-1951\(92\)90028-5](https://doi.org/10.1016/0040-1951(92)90028-5).
- Hamaguchi, H., Zana, N., Kazuo, T., Minoru, K., Masaaki, M., Sadato, U., Sawa-sawa, K., Kenji, T., 1982. Observations of volcanic earthquakes and tremors at volcanoes Nyiragongo and Nyamuragira in the Western Rift Valley of Africa. *Tohoku Geophys. J.* 29, 41–56.
- Jaupart, C., Vergnolle, S., 1989. The generation and collapse of a foam layer at the roof of a Basaltic Magma Chamber. *J. Fluid Mech.* <https://doi.org/10.1017/S0022112089001497>.
- Jones, J., Carniel, R., Harris, A.J.L., Malone, S., 2006. Seismic characteristics of variable convection at Erta 'Ale lava lake, Ethiopia. *J. Volcanol. Geotherm. Res.* 153, 64–79. <https://doi.org/10.1016/j.jvolgeores.2005.08.004>.
- Le Guern, F., 1987. Mechanism of energy transfer in the lava lake of Niragongo (Zaire), 1959–1977. *J. Volcanol. Geotherm. Res.* 31, 17–31. [https://doi.org/10.1016/0377-0273\(87\)90003-5](https://doi.org/10.1016/0377-0273(87)90003-5).
- Lev, E., Ruprecht, P., Oppenheimer, C., Peters, N., Patrick, M., Hernández, P.A., Spampinato, L., Marlow, J., 2019. A global synthesis of lava lake dynamics. *J. Volcanol. Geotherm. Res.* 381, 16–31. <https://doi.org/10.1016/j.jvolgeores.2019.04.010>.
- Mavonga, G.T., 2010. Seismic Hazard Assessment and Volcanogenic Seismicity for the Democratic Republic of Congo and Surrounding Areas, Western Rift Valley of Africa. University of the Witwatersrand, Johannesburg, South Africa.
- Michellier, C., Syavulisembo, A.M., Lagmouch, M., Kervyn, F., 2016. Limites administratives – Ville de Goma – Province du Nord-Kivu (République Démocratique du Congo). Series Pr. ed. Musée Royal de l'Afrique Centrale, Tervuren.
- Molina, I., Burgisser, A., Oppenheimer, C., 2015. A model of the geochemical and physical fluctuations of the lava lake at Erebus volcano, Antarctica. *J. Volcanol. Geotherm. Res.* 308, 142–157. <https://doi.org/10.1016/j.jvolgeores.2015.10.027>.
- Oth, A., Barrière, J., D'Oreye, N., Mavonga, G., Subira, J., Mashagiro, N., Kadufu, B., Fiam, S., Celli, G., Bigirande, J. de D., Ntenge, A.J., Habonimana, L., Bakundukize, C., Kervyn, F., 2017. KivuSNet: the first dense broadband seismic network for the Kivu Rift Region (Western Branch of East African Rift). *Seismol. Res. Lett.* 88, 49–60. <https://doi.org/10.1785/0220160147>.
- Pagliuca, N.M., Badiali, L., Cattaneo, M., Ciraba, H., Delladio, A., Demartin, M., Garcia, A., Lisi, A., Lukaya, F., Marchetti, A., Monachesi, G., Mavonga, A., Sgroi, T., Tedesco, D., 2009. Preliminary results from seismic monitoring at Nyiragongo Volcano (Democratic Republic of Congo) through telemetered seismic network, Goma volcanological observatory. *Boll. Geofis. Teor. Appl.* 50, 117–127.
- Parfitt, E.A., 2004. A discussion of the mechanisms of explosive basaltic eruptions. *J. Volcanol. Geotherm. Res.* 134, 77–107. <https://doi.org/10.1016/j.jvolgeores.2004.01.002>.
- Parfitt, E.A., Wilson, L., 1995. Modelling the transition between Hawaiian-style lava fountaining and strombolian explosive volcanic activity. *Geophys. J. Int.* 121, 226–232.
- Patrick, M., Swanson, D., Orr, T., 2019. A review of controls on lava lake level: insights from Halema'uma'u Crater, Kilauea Volcano. *Bull. Volcanol.* 81, 13. <https://doi.org/10.1007/s00445-019-1268-y>.
- Patrick, M.R., Anderson, K.R., Poland, M.P., Orr, T.R., Swanson, D.A., 2015. Lava lake level as a gauge of magma reservoir pressure and eruptive hazard. *Geology* 43, 831–834. <https://doi.org/10.1130/G36896.1>.
- Patrick, M.R., Orr, T., Sutton, A.J., Lev, E., Thelen, W., Fee, D., 2016a. Shallowly driven fluctuations in lava lake outgassing (gas pistonning), Kilauea Volcano. *Earth Planet. Sci. Lett.* 433, 326–338. <https://doi.org/10.1016/j.epsl.2015.10.052>.
- Patrick, M.R., Orr, T., Swanson, D.A., Lev, E., 2016b. Shallow and deep controls on lava lake surface motion at Kilauea Volcano. *J. Volcanol. Geotherm. Res.* 328, 247–261. <https://doi.org/10.1016/j.jvolgeores.2016.11.010>.
- Perret, F.A., 1913. The floating islands of Halemaumau. *Am. J. Sci.* <https://doi.org/10.2475/ajs.54-35.207.273>.
- Platz, T., Foley, S.F., André, L., 2004. Low-pressure fractionation of the Nyiragongo volcanic rocks, Virunga Province, D.R. Congo. *J. Volcanol. Geotherm. Res.* 136, 269–295. <https://doi.org/10.1016/j.jvolgeores.2004.05.020>.
- Sawyer, G., Carn, S.A., Tsanev, V.I., Oppenheimer, C., Burton, M., 2008. Investigation into magma degassing at Nyiragongo volcano, Democratic Republic of the Congo. *Geochim. Geophys. Geosyst.* 9, Q02017. <https://doi.org/10.1029/2007GC001829>.
- Smets, B., 2016. Dynamics of Volcanic Activity in a Youthful Extensional Setting Studied by Means of Remote Sensing and Ground-Based Monitoring Techniques: Nyiragongo and Nyamulagira Volcanoes (North Kivu, D.R. Congo). Vrije Universiteit Brussel.
- Smets, B., Delvaux, D., Ross, K.A., Poppe, S., Kervyn, M., d'Oreye, N., Kervyn, F., 2016. The role of inherited crustal structures and magmatism in the development of rift segments: insights from the Kivu basin, western branch of the East African Rift. *Tectonophysics* 683, 62–76. <https://doi.org/10.1016/j.tecto.2016.06.022>.
- Smets, B., d'Oreye, N., Kervyn, M., Kervyn, F., 2017. Gas piston activity of the Nyiragongo lava lake: first insights from a Stereographic Time-Lapse Camera system. *J. Afr. Earth Sci.* 134, 874–887. <https://doi.org/10.1016/j.jafrearsci.2016.04.010>.
- Smets, B., Oreye, N., Kervyn, F., Kervyn, M., Albino, F., Arellano, S.R., Bagalwa, M., Balagizi, C., Carn, S.A., Darrach, T.H., Fernández, J., Galle, B., González, P.J., Head, E., 2014. Detailed multidisciplinary monitoring reveals pre- and co-eruptive signals at Nyamulagira volcano (North Kivu, Democratic Republic of Congo). *Bull. Volcanol.* 76. <https://doi.org/10.1007/s00445-013-0787-1>.
- Spampinato, L., Ganci, G., Hernández, P.A., Calvo, D., Tedesco, D., Pérez, N.M., Calvari, S., Del Negro, C., Yalire, M.M., 2013. Thermal insights into the dynamics of Nyiragongo lava lake from ground and satellite measurements. *J. Geophys. Res., Solid Earth* 118, 5771–5784. <https://doi.org/10.1002/2013JB010520>.
- Swanson, D.A., Duffield, W.A., Jackson, D.B., Peterson, D.W., 1979. Chronological narrative of the 1969–71 Mauna Ulu eruption of Kilauea Volcano, Hawaii. Professional Paper. <https://doi.org/10.3133/pp1056>.
- Tazieff, H., 1984. Mt. Niragongo: renewed activity of the lava lake. *J. Volcanol. Geotherm. Res.* 20, 267–280. [https://doi.org/10.1016/0377-0273\(84\)90043-X](https://doi.org/10.1016/0377-0273(84)90043-X).
- Theys, N., De Smedt, I., Yu, H., Danckaert, T., Van Gent, J., Hörmann, C., Wagner, T., Hedelt, P., Bauer, H., Romahn, F., Pedernana, M., Loyola, D., Van Roozendaal, M., 2017. Sulfur dioxide retrievals from TROPOMI onboard Sentinel-5 Precursor: algorithm theoretical basis. *Atmos. Meas. Tech.* 10, 119–153. <https://doi.org/10.5194/amt-10-119-2017>.
- Theys, N., Hedelt, P., De Smedt, I., Lerot, C., Yu, H., Vlietinck, J., Pedernana, M., Arellano, S., Galle, B., Fernandez, D., Carlito, C.J.M., Barrington, C., Taisne, B., Delgado-Granados, H., Loyola, D., Van Roozendaal, M., 2019. Global monitoring of volcanic SO<sub>2</sub> degassing with unprecedented resolution from TROPOMI onboard Sentinel-5 Precursor. *Sci. Rep.* 9. <https://doi.org/10.1038/s41598-019-39279-y>.
- Valade, S., Ripepe, M., Giuffrida, G., Karume, K., Tedesco, D., 2018. Dynamics of Mount Nyiragongo lava lake inferred from thermal imaging and infrasound array. *Earth Planet. Sci. Lett.* 500, 192–204. <https://doi.org/10.1016/j.epsl.2018.08.004>.
- Vergnolle, S., Jaupart, C., 1990. Dynamics of degassing at Kilauea Volcano, Hawaii. *J. Geophys. Res., Solid Earth* 95, 2793–2809. <https://doi.org/10.1029/JB095iB03p02793>.
- Waldhauser, F., Ellsworth, W.L., 2000. A double-difference earthquake location algorithm: method and application to the Northern Hayward Fault, California. *Bull. Seismol. Soc. Am.* 90, 1353–1368. <https://doi.org/10.1785/0120000006>.
- Woods, J., Donaldson, C., White, R.S., Caudron, C., Brandsdóttir, B., Hudson, T.S., Ágústsdóttir, T., 2018. Long-period seismicity reveals magma pathways above a laterally propagating dyke during the 2014–15 Bárðarbunga rifting event, Iceland. *Earth Planet. Sci. Lett.* 490, 216–229. <https://doi.org/10.1016/j.epsl.2018.03.020>.
- Worster, M.G., Huppert, H.E., Sparks, R.S.J., 1993. The crystallization of lava lakes. *J. Geophys. Res., Solid Earth* 98, 15891–15901. <https://doi.org/10.1029/93JB01428>.
- Xu, Y., Koper, K.D., Burlacu, R., 2017. Lakes as a source of short-period (0.5–2 s) microseisms. *J. Geophys. Res., Solid Earth* 122, 8241–8256. <https://doi.org/10.1002/2017JB014808>.